Foundation for the support of this research. D.R.T. acknowledges the Alfred P. Sloan Foundation for a Fellowship.

Supplementary Material Available: Experimental section for the crystal structure analysis and tables of atomic coordinates and isotropic or equivalent isotropic thermal parameters, bond angles, crystallographic information, nonbonded contact distances, calculated coordinates and thermal parameters for hydrogen atoms, anisotropic thermal parameters, torsion angles, and least-squares planes (14 pages); tables of observed and calculated structure factor amplitudes (13 pages). Ordering information is given on any current masthead page.

Electronic Origin for the Geometric Preferences of $HM_3(CO)_{10}(\mu$-CR) Compounds

Eluvathingal D. Jemmis* and Bharatam V. Prasad†

School of Chemistry, University of Hyderabad, Central University P.O., Hyderabad, 500 134 India

Received September 27, 1990

The electronic factors that control the variation of the bridging carbyne unit in $HM_3(CO)_{10}(\mu$-CR) from μ_2 to μ_3 have been studied by extended Huckel calculations on the models $HFe_3(CO)_{10}(\mu$-CR) (**3a**, R = H; **3b**, R = NH_2) and $HFe_3(CO)_{10}(\mu$-COMe) (III). The HOMO-1 of **3a** (and of **3b** and III) has antibonding character between the p orbital of carbyne and all the three metals. Substituents on the carbynyl carbon influence the metal–carbon antibonding interaction, but not equally with all metals. This delicate balance of antibonding interactions leads to a variation in the dihedral angle θ between the M–M–M plane and the M–C–M plane as a function of R. Molecular orbital patterns indicate only the μ_2 arrangement for carbyne in all $HM_3(CO)_{10}(\mu$-CR) compounds. In $HOs_3(CO)_{10}(\mu$-CH) (XXI) the C–H bond is η^2-μ_2 bridging but not μ_3 bridging. The μ_3 arrangement of carbyne in $HM_2M'(CO)_7Cp(\mu$-CR) is due to the directionality of the MOs of the M(CO)Cp unit.

Introduction

Carbyne (CR) ligands appear in organometallic chemistry with metal attachments ranging from one to four (μ_1–μ_4).[1] μ_1, μ_2, and μ_3 bridging carbyne arrangements are in principle possible with a trinuclear carbyne complex. There has been no characterized example of a monohapto (μ_1) carbyne ligand attached to a trinuclear cluster. The μ_3 carbyne bridging mode is well-known in the trinuclear complexes 1,[1c] isolobal to tetrahedrane. μ_2-CR on tri-

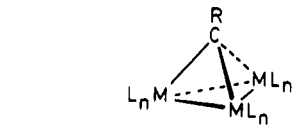

1

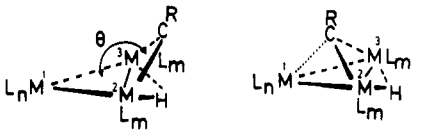

2a 2b

metallic templates presents a different story.[2-25] A perusal of available structures (Table I) indicates that the μ_2-CR attachment is a very delicate one. With changes in the substituent R, the CR group can shift gradually from a μ_2 to a μ_3 position. The electronic factors that control such a gradation are discussed in this contribution.

All structures of type **2** (listed in Table I) have 48 valence electrons, same as that in **1**. However, their geometries are very different. At one extreme these could be described as the bicyclobutane-like structure **2a** where the

Table I. Structures of Trinuclear Carbyne Complexes (I–XXVIII) along with the M(1)–C Distance (Å) and Dihedral Angle θ (deg)

compd	no.	M(1)–C	θ	ref
$HFe_3(CO)_{10}(\mu$-CO)$^-$	I	3.00	102.0	2a
$HFe_3(CO)_{10}(\mu$-$CNMe_2)$	II	2.89	96.8	3e
$HFe_3(CO)_{10}(\mu$-COMe)	III	2.70	91.0	2a
$HFe_3(CO)_{10}(\mu$-COH)	IV			4
$HFe_3(CO)_{10}(\mu$-$CCH_3)$	V			5
$HFe_3(CO)_{10}(\mu$-CH)	VI			6
$HRu_3(CO)_{10}(\mu$-CO)$^-$	VII	3.17	102.4	7
$HRu_3(CO)_{10}(\mu$-$CNMe_2)$	VIII	3.08	100.4	8
$HRu_3(CO)_{10}(\mu$-COMe)	IX	2.90	94.4	9
$HRu_3(CO)_{10}(\mu$-COH)	X			10
$HRu_3(CO)_9Py(\mu$-$CNBz_2)$	XI			11b
$HRu_3(CO)_9PPh_3(\mu$-$CNBz_2)$	XII			11b
$HRu_3(CO)_{10}(\mu$-$COBH_2NMe_3)$	XIII	2.96	95.8	12
$HRu_3(CO)_{10}(\mu$-CH)	XIV			13
$HOs_3(CO)_{10}(\mu$-COMe)	XV			14
$HOs_3(CO)_{10}(\mu$-$CNMe_2)$	XVI			15
$HOs_3(CO)_{10}(\mu$-CPh)	XVII	2.59	78.2	16
$HOs_3(CO)_{10}(\mu$-$CCH{=}CH_2)$	XVIII			17
$HOs_3(CO)_{10}(\mu$-$CCH_3)$	XIX			18
$HOs_3(CO)_{10}(\mu$-$CCH_2CHMe_2)$	XX	2.64	82.1	17
$HOs_3(CO)_{10}(\mu$-CH)	XXI	2.35	69.7	19
$HRhFe_2Cp(CO)_7(\mu$-COMe)	XXII	2.21	69.2	20
$HCoFe_2Cp(CO)_7(\mu$-COMe)	XXIII	2.00	64.7	21
$NiFe_2Cp(CO)_7(\mu$-COMe)	XXIV	1.96		21
$(AuPPh_3)M_3(CO)_{10}(\mu$-COMe)[a]	XXV			22
$(AuPPh_3)Fe_2CoCp(CO)_7(\mu$-COMe)	XXVI	1.93		21
$HOs_3(CO)_9(\mu$-CPh)[=C$(OMe)_2$]	XXVII	2.29	66.6	14b
$HOs_3(CO)_{10}(\mu$-C[PhC=C=C(Ph)-Re$(CO)_4PMe_2Ph$])	XXVIII	3.09	99.1	23

[a] M = Fe, Ru.

† Present address: Department of Chemistry, University of Alabama at Birmingham, Birmingham, AL 35205.

0276-7333/91/2310-3613$02.50/0

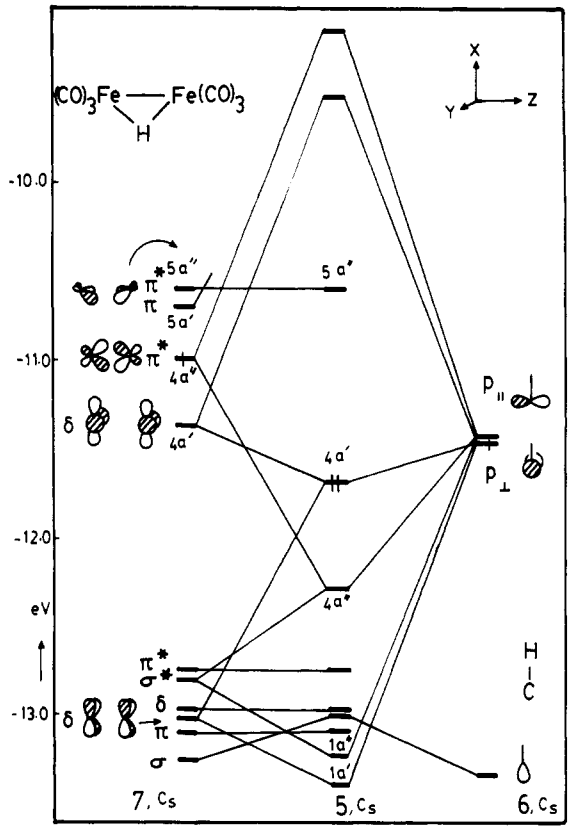

Figure 1. Interaction diagram for the construction of the MOs of the fragment $Fe_2(CO)_6(\mu\text{-}H)(\mu\text{-}CH)$ (**5**) from smaller fragments CH (**6**) and $Fe_2(CO)_6(\mu\text{-}H)$ (**7**).

angle θ between the M(1)–M(2)–M(3) plane and the M(2)–C–M(3) plane is much larger than 90° (VIII, Table I).[8]

This leaves no possibility for M(1)–CR bonding. If one assumes that the 4 electrons (3 from CR and 1 from H) donated to the bridge are equally shared by M(2) and M(3), all the three metals in **2a** would satisfy the 18-electron rule. At the other extreme we have compound, XXIII (Table I), where θ is as small as 64.7° (representing **2b**).[21] This leads to an M(1)–CR distance of about 2.0 Å, which is clearly within the bonding range. A conventional electron count that demands the carbyne to be a 3-electron donor (1 electron to each metal) leads to the electron counts M(1) = 19 and M(2) = M(3) = 17.5 in **2b**. A charge-separated structure where M(1) holds +1 and M(2) and M(3) have $-^1/_2$ each brings back the 18-electron count. This does not provide any better understanding of the electronic structure of the system, especially when one considers the fact that the structure is controlled by the substituent R on the carbynyl carbon.

With electron-donating substituents on the carbynyl carbon, the angle θ is large (as large as 102° when R = O^-, VII, Table I). As the electron-donating capacity of the R group decreases, θ and the M(1)–C distance decrease. This can be clearly observed in Table I (I–III, Fe complexes; VII–IX and XIII, Ru complexes; XVII, XX, and XXI, Os complexes). When R is replaced by hydrogen (in XXI, Table I), θ is less than 70° and a semi-triply bridging nature

(1) (a) Here, alkylidynes are referred as μ_1-CR complexes. A recent review dealing with the chemistry of alkylidynes: Kim, H. P.; Angelici, R. J. *Adv. Organomet. Chem.* **1987**, *27*, 51. (b) Many compounds with μ_2-carbyne bridges are known. Two articles that give most of the references: Holton, J.; Lappert, M. F.; Rearce, R.; Yarrow, P. I. W. *Chem. Rev.* **1983**, *83*, 135. Jemmis, E. D.; Prasad, B. V. *Polyhedron* **1988**, *7*, 871. (c) Recent references on μ_3-carbyne-bridged trinuclear transition-metal compounds: Penfold, B. R.; Robinson, B. H. *Acc. Chem. Res.* **1973**, *6*, 73. Seyferth, D. *Adv. Organomet. Chem.* **1973**, *6*, 73. Mingos, D. M. P. *Adv. Organomet. Chem.* **1977**, *15*, 1. Wijeyesekera, S. D.; Hoffmann, R. *Organometallics* **1984**, *3*, 949. Shilling, B. E. R.; Hoffmann, R. *J. Am. Chem. Soc.* **1979**, *101*, 3456. (d) Important review dealing with the μ_4-CR bridged complexes: Bradley, J. S. *Adv. Organomet. Chem.* **1976**, *14*, 98.

(2) (a) Shriver, D. F.; Lehman, D.; Strope, D. *J. Am. Chem. Soc.* **1975**, *97*, 1594. (b) Keister, J. B. *J. Chem. Soc., Chem. Commun.* **1979**, 214. (c) Sumner, C. E., Jr.; Collier, J. A.; Pettit, R. *Organometallics* **1982**, *1*, 1350.

(3) (a) Rhee, I.; Ryang, M.; Tatsumi, S. *Chem. Commun.* **1968**, 455. (b) Greatrex, R.; Greenwood, N. N.; Rhee, I.; Ryang, M.; Tatsumi, S. *Chem. Commun.* **1970**, 1193. (c) Altman, J.; Welcman, N. *J. Organomet. Chem.* **1979**, *165*, 353. (d) Howell, J. A. S.; Mathur, P. *J. Chem. Soc., Dalton Trans.* **1982**, *43*. (e) Herbstein, F. H. *Acta. Crystallogr.* **1981**, *B37*, 339.

(4) Hodali, H. A.; Shriver, D. F.; Ammlung, C. A. *J. Am. Chem. Soc.* **1978**, *100*, 5239.

(5) Vites, J.; Fehlner, T. P. *Organometallics* **1984**, *3*, 491.

(6) A μ_2-arrangement with small dihedral angle θ may be expected for $HFe_3(CO)_{10}(\mu\text{-}CH)$ from the experimental and spectral details. Kolis, J. W.; Holt, E. M.; Shriver, D. F. *J. Am. Chem. Soc.* **1983**, *105*, 7307.

(7) Johnson, B. F. G.; Lewis, J.; Raithby, P. R.; Suss, G. *J. Chem. Soc., Dalton Trans.* **1979**, 1356.

(8) (a) Churchill, M. R.; DeBoer, B. G.; Rotella, F. J.; Abel, E. W.; Rowley, R. J. *J. Am. Chem. Soc.* **1975**, *97*, 7158. (b) Abel, E. W.; Farrow, G. W. *J. Inorg. Nucl. Chem.* **1980**, *42*, 541. (c) Churchill, M. R.; DeBoer, B. G.; Rotella, F. J. *Inorg. Chem.* **1976**, *15*, 1843. (d) Adams, R. D.; Babin, J. E.; Tanner, J. *Organometallics* **1988**, *7*, 765.

(9) (a) Johnson, B. F. G.; Lewis, J.; Orpen, A. G.; Raithby, P. R.; Suss, G. *J. Organomet. Chem.* **1979**, *173*, 187. (b) Churchill, M. R.; Beanan, L. R.; Wassermann, H. J.; Bueno, C.; Rahman, Z. A.; Keister, J. B. *Organometallics* **1983**, *2*, 1179.

(10) Nevinger, L. R.; Keister, J. B.; Maher, J. *Organometallics* **1990**, *9*, 1900.

(11) Ligand substitutional isomerism on these complexes is studied. (a) Dalton, D. M.; Barnett, D. J.; Duggan, T. P.; Keister, J. B.; Malik, P. T.; Modi, S. P.; Shaffer, M. R.; Smesko, S. A. *Organometallics* **1985**, *4*, 1854. (b) Churchill, M. R.; Fettinger, J. C.; Keister, J. B. *Organometallics* **1985**, *4*, 1867.

(12) Chipperfield, A. K.; Housecroft, C. E.; Raithby, P. R. *Organometallics* **1990**, *9*, 479.

(13) Holmgren, J. S.; Shapley, J. R. *Organometallics* **1984**, *3*, 1322.

(14) Hodali, H. A.; Shriver, D. F. *Inorg. Chem.* **1979**, *18*, 1236.

(15) (a) Adams, R. D.; Babin, J. E.; Kim, H.-S. *Polyhedron* **1988**, *7*, 967. (b) Adams, R. D.; Babin, J. E.; Kim, H.-S. *Organometallics* **1987**, *6*, 749. (c) Adams, R. D.; Babin, J. E. *Inorg. Chem.* **1987**, *26*, 980.

(16) (a) Yeh, W.-Y.; Shapley, J. R.; Li, Y.-J.; Churchill, M. R. *Organometallics* **1985**, *4*, 767. (b) Yeh, W.-Y.; Kneuper, H.-J.; Shapley, J. R. *Polyhedron* **1988**, *7*, 961. (c) Shapley, J. R.; Yeh, W.-Y.; Churchill, M. R.; Li, Y-J. *Organometallics* **1985**, *4*, 1898.

(17) Green, M.; Orpen, A. G.; Schaverein, C. J. *J. Chem. Soc., Chem. Commun.* **1984**, 37.

(18) Went, M. J.; Sailor, M. J.; Bogdan, P. L.; Borck, C. P.; Shriver, D. F. *J. Am. Chem. Soc.* **1987**, *109*, 6023.

(19) Shapley, J. R.; Cree-Uchiyama, M. E.; George, G. M. St.; Churchill, M. R.; Bueno, C. *J. Am. Chem. Soc.* **1983**, *105*, 140.

(20) Farrugia, L. J. *J. Organomet. Chem.* **1986**, *310*, 67.

(21) Aitchison, A. A.; Farrugia, L. J. *Organometallics* **1986**, *5*, 1103.

(22) Bateman, L. W.; Green, M.; Mead, K. A.; Mills, R. M.; Salter, I. D.; Stone, F. G. A.; Woodward, P. *J. Chem. Soc., Dalton Trans.* **1983**, 2599.

(23) (a) Koridze, A. A.; Kizas, O. A.; Kolobova, N. E.; Petrovskii, P. V. *J. Organomet. Chem.* **1985**, *292*, C1. (b) Koridze, A. A.; Kizas, O. A.; Kolobova, N. E.; Yanovsky, A. I.; Struchkov, Yu. T. *J. Organomet. Chem.* **1986**, *302*, 413.

(24) The chemistry of the compounds with the general formula $HM_3(CO)_{10}(\mu\text{-}CR)$ including the spectra, kinetics, oxidative addition, reductive elimination, alkyne coupling, photochemistry, metal-exchange reactions, etc. are discussed in the following references: (a) Adams, R. D. *Chem. Rev.* **1989**, *89*, 1703. (b) Deeming, A. J. *Adv. Organomet. Chem.* **1986**, *26*, 1. (c) Teller, R. G.; Bau, R. *Struct. Bonding (Berlin)* **1981**, *44*, 1. (d) Beanan, L. R.; Rahman, Z. A.; Keister, J. B. *Organometallics* **1983**, *2*, 1062. (e) Iskola, E.; Pakkanen, T. A.; Pakkanen, T. T.; Venalainen, T. *Acta Chem. Scand.* **1983**, *A37*, 125. (f) Gavens, P. D.; Mays, M. J. *J. Organomet. Chem.* **1978**, *162*, 389. (g) Keister, J. B. *Polyhedron* **1988**, *7*, 847. (h) Beanan, L. R., Keister, J. B. *Organometallics* **1985**, *4*, 1713. (i) Bavaro, L. M.; Montangerro, P.; Keister, J. B. *J. Am. Chem. Soc.* **1983**, *105*, 4977. (j) Jungbluth, H.; Suss-Fink, G.; Pellighelli, M. A.; Tiripicchio, A. *Organometallics* **1989**, *8*, 925. (k) Bavaro, L. M.; Keister, J. B. *J. Organomet. Chem.* **1985**, *287*, 357. (l) Friedman, A. E.; Ford, P. C. *J. Am. Chem. Soc.* **1989**, *111*, 551. (m) Keister, J. B.; Payne, M. W.; Muscatella, M. J. *Organometallics* **1983**, *2*, 219. (n) Keister, J. B.; Onyeso, C. C. O. *Organometallics* **1988**, *7*, 2364.

(25) There are some more examples where a carbyne is μ_2 bridging in trimetallic clusters but which do not come into the general formula under discussion. (a) Chi, Y.; Shapley, J. R. *Organometallics* **1985**, *4*, 1900. (b) Adams, R. D.; Babin, J. E.; Kim, H.-S. *Organometallics* **1987**, *6*, 749. (c) Delgado, E.; Jeffery, J. C.; Stone, F. G. A. *J. Chem. Soc., Dalton Trans.* **1986**, 2105.

of the CH group is suggested on the basis of distances.[19] What is the electronic origin for this change of θ as a function of R? What is the actual bridging nature of the carbyne (CR) group in this series of complexes? At small values of θ (70°) can the CR group be described as μ_3? Is there any π delocalization in the M(2)–C–M(3) plane? How do the substituents dictate the redistribution of charge implied in the electron count? The bulkiness of the R group does not appear to control the angle θ. It has been suggested that the metal M(1) donates electrons to the π^* orbital of C–OMe or C–NMe_2 bridging groups.[3d] But a conventional electron count demands localization of extra charge on M(2) and M(3) and not on CR.

Replacement of the $M(1)(CO)_4$ unit in **2** by isoelectronic Cp(CO)Rh or Cp(CO)Co units (XXII or XXIII, Table I) leads to a μ_3 arrangement for the carbyne ligand, with a short M(1)–C distance, even with an electron-donating R.[20,21] Is it possible that the origins of the short M(1)–C distance in $HM_3(CO)_{10}(\mu$-CR) and in $HM_2M'Cp(CO)_7(\mu$-CR) are different? There are several examples in literature where short interatomic distances do not represent bonding interactions.[26] Are the compounds under discussion further examples of this?[27]

In this paper, we have tried to understand the electronic origin of the variation of θ as a function of the substituent (R) on the bridging carbyne (CR) in **2**. The electronic structure of the model compound $HFe_3(CO)_{10}(\mu$-CH) (**3a**)

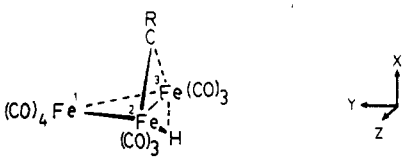

3a R = H
3b R = NH_2

is studied first to understand the various molecular orbital interactions present in this series of molecules. Electronic structures of $HFe_3(CO)_{10}(\mu$-COMe) and $HFe_3(CO)_{10}(\mu$-CNH_2) are studied as representatives of **2a**. Walsh diagrams are constructed to delineate the variation in the MOs as a function of θ. The electronic structure of $HOs_3(CO)_{10}(\mu$-CH) (XXI) is studied to explain its preferences for smaller values of θ. The MO pattern of $HRhFe_2Cp(CO)_7(\mu$-CH) is also studied to explain the μ_3 arrangement of the CR bridge in XXII and XXIII. The fragment molecular orbital approach[28] within the extended Huckel method[29] is used in these studies.

Results and Discussion

Electronic Structure of $HFe_3(CO)_{10}(\mu$-CH)[6] (3a). $HFe_3(CO)_{10}(\mu$-CH) (**3a**) in which the dihedral angle, θ, formed by the two planes Fe(1)–Fe(2)–Fe(3) and Fe(2)–C–Fe(3), kept at 90° is taken as a model to understand the molecular orbital pattern of the complexes of type **2**. The

Scheme I

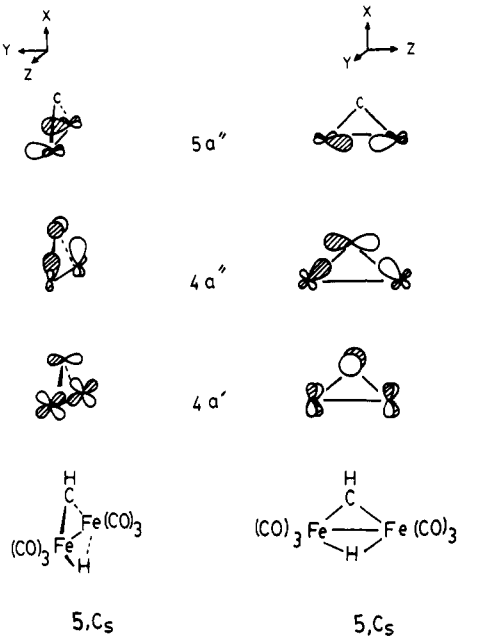

5,C_s 5,C_s

details of atomic and geometric parameters used in the calculations are given in the Appendix. The molecular orbitals of **3a** are constructed from the MOs of the smaller fragments $Fe(CO)_4$ (**4**) and $HFe_2(CO)_6(\mu$-CH) (**5**). The MOs of fragment **5**, in turn, are constructed from those of the methylidyne group, **6**, and of the remaining fragment $HFe_2(CO)_6$ (**7**) (Figure 1). The carbyne group has a σ orbital and two unhybridized p orbitals, one in the plane of the fragment **5** ($p_\parallel$) and the other out of the plane ($p_\perp$). The important orbitals 3a′ (δ), 4a′ (δ), 4a″ (π^*), and 5a″ (π^*) of fragment **7** are shown in Figure 1. Mulliken symbols σ, π, and δ, should not be taken literally here, as the low symmetry of the system results in considerable mixing amongst them. Figure 1 shows that major interactions between fragments **6** and **7** lead to the HOMO-1 of **5**. 5a″ (π^*) of fragment **7** does not find any match in the orbitals of **6** and becomes the LUMO (5a″) of **5**. 4a″ (π^*) of **7** interacts with $p_\parallel$ of **6** to give 4a″ of **5**, corresponding to the formation of M–C (σ) bonds. 1a′ of **5** is a π MO delocalized over Fe(2)–C–Fe(3). 4a′ (HOMO) is the corresponding antibonding combination obtained from a three-center 4-electron interaction between 3a′ (δ) and 4a′ (δ) of **7** and $p_\perp$ of CH. In 4a′ of **5**, $p_\perp$ of carbyne has a bonding interaction with one of the M(2)–M(3) δ bonds and an antibonding interaction with another (Figure 1). M(2)–C–M(3) π delocalization should not be expected in fragment **5** because both 1a′ and 4a′ are occupied. The presence of 4 π electrons prompts us to consider the fragment **5** to be analogous to the cyclopropenyl anion.[30] The three orbitals 4a′, 4a″, and 5a″ of **5** are important for further discussion and are drawn in Scheme I.

Interaction of fragment $HFe_2(CO)_6(\mu$-CH) (**5**) with the familiar $Fe(CO)_4$ fragment[31] gives **3a**. The interaction diagram (Figure 2, left) shows that HOMO–LUMO interactions lead to metal–metal bonds, 6a′ and 6a″. 4a″ of fragment **5** becomes the HOMO-2 (5a″) of **3a**. The remaining interactions are of the two-center, 4-electron (2c–4e) kind and do not contribute to the bonding. The important molecular orbitals (1a′, 3a′, and 6a′) of **3a** are

(26) (a) In metal allyl interaction the central carbon of the allyl group does not show any bonding interaction, but the M–C distance is always within the bonding range. Clark, T.; Jemmis, E. D.; Schleyer, P.v.R.; Binkley, J. S.; Pople, J. A. *J. Organomet. Chem.* **1978**, *150*, 1. Setzer, W. N.; Schleyer, P.v.R. *Adv. Organomet. Chem.* **1985**, *24*, 353. (b) M–M bonding distances are observed in several compounds, but the MO pattern precludes the possibility of M–M bonding interaction. Fink, M. J.; Haller, K. J.; West, R.; Michl, J. *J. Am. Chem. Soc.* **1984**, *106*, 822. Bottomley, F. *Inorg. Chem.* **1983**, *22*, 2656.

(27) The fact that the novel $M_3(CO)_{10}$ compounds are the original precursors for this series of compounds enhances the interest in these compounds. (a) Dahl, L. R.; Blount, J. F. *Inorg. Chem.* **1965**, *4*, 1373. (b) Cotton, F. A.; Troup, J. M. *J. Am. Chem. Soc.* **1974**, *96*, 4155.

(28) Fujimoto, H.; Hoffmann, R. *J. Phys. Chem.* **1974**, *78*, 1167.

(29) (a) Hoffmann, R.; Lipscomb, W. N. *J. Chem. Phys.* **1962**, *36*, 2179. (b) Hoffmann, R. *J. Chem. Phys.* **1963**, *39*, 1397.

(30) The possibility of considering the M–C(R)–M ring as an anion was suggested previously by Howell and Mathur in ref 3d.

(31) Albright, T. A.; Burdett, J. K.; Whangbo, M. H. *Orbital Interactions in Chemistry*; John Wiley & Sons: New York, 1984; p 412.

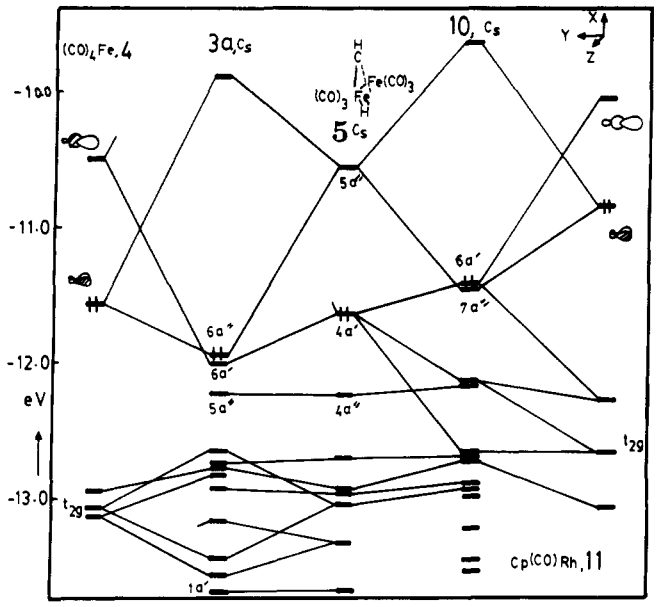

Figure 2. Diagram showing the interaction of fragment $HFe_2(CO)_6(\mu\text{-CH})$ (**5**) (left) with $Fe(CO)_4$ to give $HFe_3(CO)_{10}(\mu\text{-CH})$ (**3**) and (right) with Rh(CO)Cp to give $HRhFe_2(CO)_7Cp(\mu\text{-CH})$ (**10**) (at $\theta = 90°$).

Scheme II

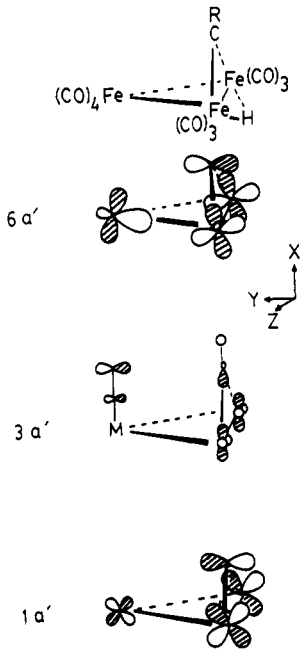

shown in Scheme II. The 1a′ orbital of **3a** corresponds to Fe(2)–C–Fe(3) π delocalization. In addition to this interaction, the carbynyl carbon has a bonding interaction with Fe(1) in the 1a′ MO. The 6a′ orbital (HOMO-1) has antibonding interaction between the $p_\perp$ orbital of carbyne and all the three metals, but these antibonding interactions are not equal in magnitude. The interaction of the p orbital of the CR group within the Fe(2)–Fe(3) fragment is through an Fe(2)–Fe(3) δ orbital (can be described as π^*) while the interaction with Fe(1) may be described as σ^*. In 3a′ there is an antibonding interaction between one of the carbonyls on Fe(1) and the C–H bond of the bridging group. 6a″ is an M–M bonding orbital.

The Fe(1)–Fe(2) and Fe(1)–Fe(3) overlap populations are 0.14 each and the Fe(2)–Fe(3) overlap population is 0.04 in **3a**. This indicates that the σ bond between Fe(2) and Fe(3) is very weak. A thorough analysis of the MOs

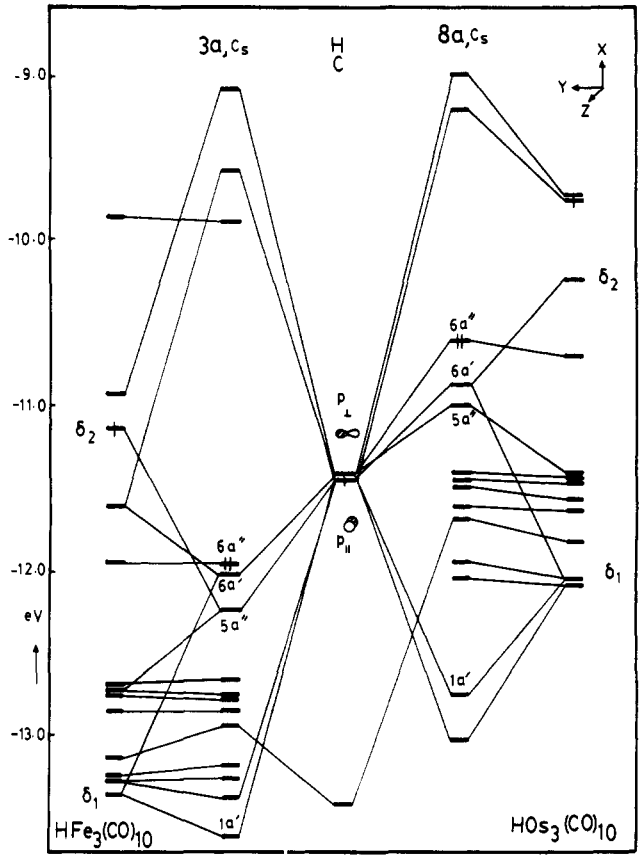

Figure 3. Interaction diagram showing interaction of bridging CH with the remaining fragment (left) leading to $HFe_3(CO)_{10}(\mu\text{-CH})$ (**3a**) and (right) leading to $HOs_3(CO)_{10}(\mu\text{-CH})$ (**8a**).

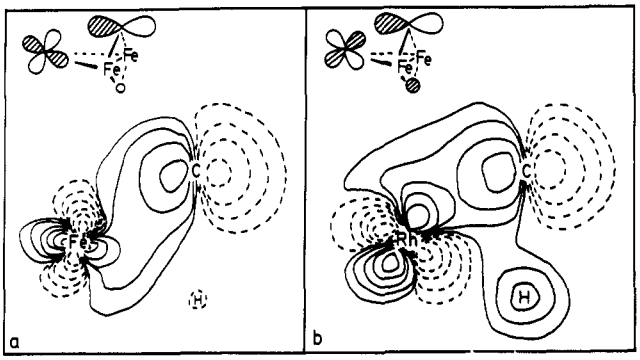

Figure 4. Contour plots showing the M(1) and C(H) interaction in HOMO-1 (a) in $HFe_3(CO)_{10}(\mu\text{-CH})$ (**3a**) and (b) in $HRhFe_2Cp(CO)_7(\mu\text{-CH})$ (**9**), both at $\theta = 90°$.

suggests that there is a three-center 2-electron bond in the Fe(2)–H–Fe(3) framework. In this context, the bridging hydrogen may be treated as H^+ with a negative charge in the Fe(2)–C–Fe(3) ring.[3d] The Fe(2)–C and Fe(3)–C bonds are regular 2-center 2-electron bonds, which leaves 4 π electrons (one each from CR, Fe(2), and Fe(3)[32] and one because of the negative charge in the Fe(2)–C–Fe(3) ring) to be distributed in the Fe(2)–C–Fe(3) framework. They are found in the 1a′ (π) and 6a′ (π^*) orbitals of **3a**.

To understand the nature of the MOs of **3a** in detail, the interaction diagram between $HFe_3(CO)_{10}$ and CH is also studied (Figure 3, left). The 6a′ orbital of **3a** is a result

(32) The $Fe(CO)_3$ group is considered to be donating one electron to the π frame of Fe(2)–C–Fe(3) in the following way. $Fe(CO)_3$ is a 14-electron unit. The 3c–2e bond with H has 1 electron. It shares an electron in the bond with $Fe(CO)_4$ and another with the bridging carbon in a π bond. The 18th electron is placed in the Fe(2)–C–Fe(3) π frame.

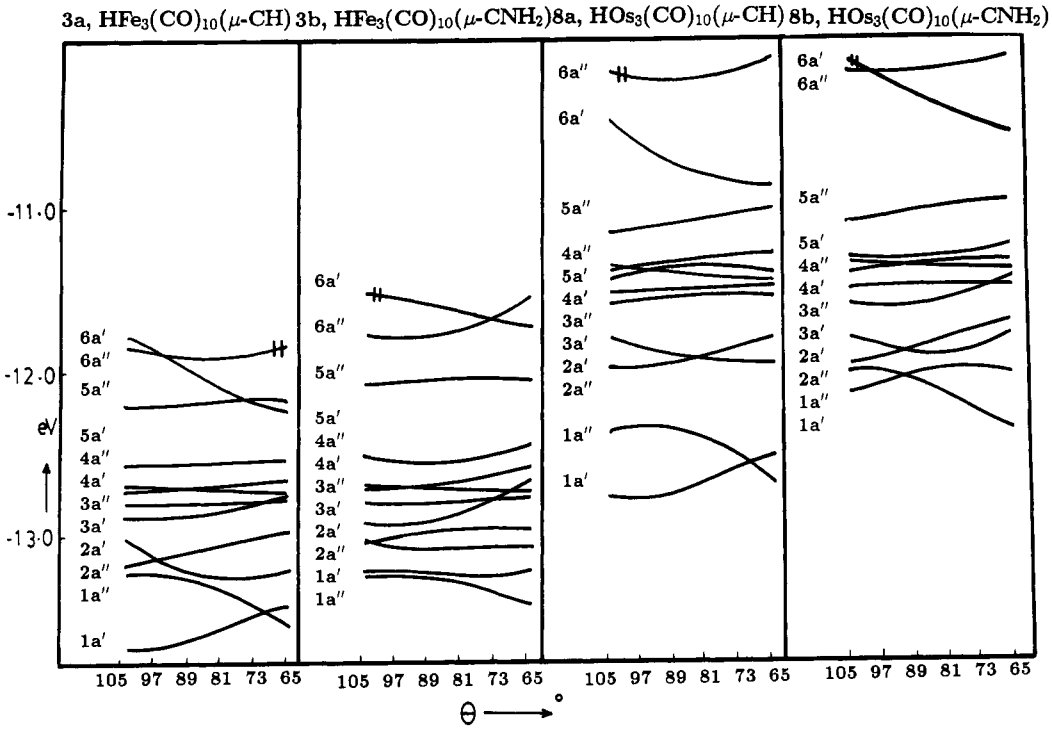

Figure 5. Walsh diagrams showing the variation in the MO pattern of (a) $HFe_3(CO)_{10}(\mu\text{-}CH)$, (b) $HFe_3(CO)_{10}(\mu\text{-}CNH_2)$, (c) $HOs_3(CO)_{10}(\mu\text{-}CH)$, and (d) $HOs_3(CO)_{10}(\mu\text{-}CNH_2)$ as a function of a variation in the M(1)–M(2)–M(3) and M(2)–C–M(3) dihedral angles θ.

of the 3c–4e interaction between δ_1 and δ_2 of $HFe_3(CO)_{10}$ and the p orbital of CH. The p orbital finds antibonding interaction with d_{xy}–d_{xy} δ (δ_1) and bonding interaction with $d_{x^2-y^2}$–$d_{x^2-y^2}$ δ (δ_2). This causes a delicate balance between bonding and antibonding interactions in 6a′ of **3a**. The MO diagram shows only an antibonding interaction with all the three metals (Figure 4a shows the contour plot for 6a′ in the Fe(1)–C(H) plane). Both bonding and antibonding combinations 1a′ (σ), 1a″ (π), 2a″(π^*), and 6a′ (σ^*) between Fe (1) and C are occupied. There is no net effective π delocalization in Fe(2)–C–Fe(3) as both the π (1a′) and π^* (6a′) MOs are occupied. The HOMO has insignificant contribution from the CR bridge.

A Walsh diagram (Figure 5a) is constructed to understand the variations in the MO pattern as a function of dihedral angle θ for the molecule **3a**. The geometric details are given in the Appendix. The curve for the sum of the 1-electron energies shows a minimum at 77°. A major contribution comes from the 6a′ orbital, which steeply decreases in energy. This is mainly due to the decrease in the Fe(2)–C–Fe(3) π^* interaction. With a decrease in θ, the antibonding interaction (σ^*) between the $p_\perp$ orbital of carbon and d_{xy} of Fe(1) increases. As a result, the slope of 6a′ decreases at low dihedral angles. Variation in the sum of 1-electron energies directly follows the variation of 6a′, except for the increase in the energy due to steric factors (as shown by the 3a′ orbital). 3a′ increases in energy at small dihedral angles because of the development of antibonding interactions between the carbonyl group on Fe(1) and hydrogen on carbynyl group (Scheme II). The variations in the remaining MOs contribute minimally to the variation in the sum of 1-electron energies. As the dihedral angle decreases from 105 to 65°, some bonding interactions (1a′, 1a″) are developed between Fe(1) and the carbynyl carbon but these are at the cost of bonding interactions already existing between Fe(2) and C and Fe(3) and C, as in 1a′. The newly developing bonding interactions between Fe(1) and C are offset by the developing antiboding interactions, as in the 1a′, 6a′ pair and the 1a″, 6a″ pair. The overlap population between Fe(1) and C is only slightly increased (0.053 at θ = 90° and 0.061 at θ = 77°), and this cannot be taken as evidence for increased Fe(1)–CR bonding interaction. The σ^* interaction between Fe(1) and C(H) in 6a′ increases with decreasing θ. Therefore the Fe(1)–C bond should not be expected at small θ. Even though the Fe(1)–C distance (2.42 Å) indicates a μ_3 bridge (at θ = 77°), on the basis of MO pattern and overlap population analysis, we should consider the carbyne as only a μ_2 rather than a μ_3 bridge in VI.[6] From the Walsh diagram (Figure 5a) it is clear that the antibonding interaction between the carbon $p_\perp$ orbital and the δ orbital on Fe(2)–Fe(3) (6a′, Scheme II) is responsible for the preference of the structure with the low dihedral angle.[6,13,19]

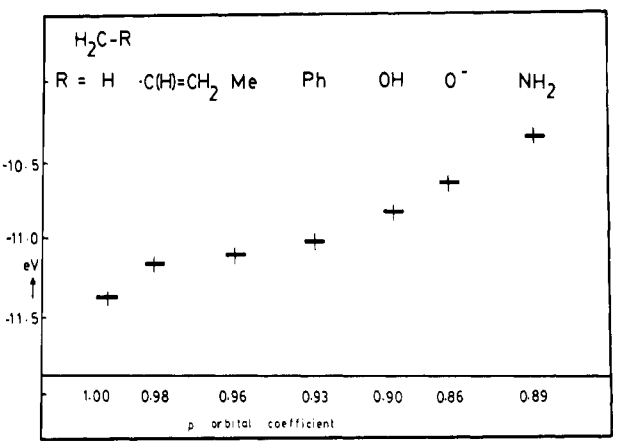

Figure 6. Correlation diagram showing the variation of the energy of p orbital as a function of R in H_2CR.

Electronic Structure of $HFe_3(CO)_{10}(\mu\text{-}COMe)$ (III)[2a] and Effect of the Substituent on the Carbynyl Carbon. The angle θ is found to increase with the electron-donating capacity of the substituent R (Table I). What is the electronic origin of this behavior? Figure 6 shows

the energy level pattern of the orbitals of carbon in H_2CR as a function of R. The unhybridized p orbital is pushed up in energy as we go along the range R = H, CH = CH_2, CH_3, Ph, OH, O^-, and NH_2. At the same time, the p orbital coefficient on carbon decreases in the same order. These effects are mainly due to the participation of the pseudo p orbital of the R group in an antibonding interaction (π^*) with the p orbital of H_2CR. The stronger the participation, the more the destabilization.

In the HOMO-1 (6a′) of **3a**, the p orbital of carbyne has antibonding interaction with all the three metals. From the Walsh diagram (Figure 5a) it is clear that 6a′ controls the sum of 1-electron energies. If the antibonding interaction between CR and Fe(2)–C–Fe(3) is very strong, the CR would shift toward Fe(1), decreasing θ. On the other hand if this interaction is weak, the Fe(1)–CR antibonding takes over, increasing θ. The M(2)–C–M(3) π^* interaction is considerably less with electron-donating R groups because of the smaller coefficient size, and the decrease in θ decreases the M(2)–C–M(3) π^* interaction. This antibonding interaction is considerably less with electron-donating R groups because of the smaller coefficient size and higher energy of the p orbital of C(R). Since the antibonding interaction is low to start with, it is not necessary to have smaller values of θ. As a result, the compounds with an electron-donating R can accommodate larger dihedral angles.

Extended Huckel calculations are performed on $HFe_3(CO)_{10}(\mu\text{-COMe})$ (III).[2a] The MO pattern of III is very very similar to that of **3a** except for small changes in the MO energies. The HOMO-1 of III also has an antibonding interaction between the $p_\perp$ orbital of the CR group with σ of Fe(2)–Fe(3) (π^*) and d_{xy} of Fe(1) (σ^*). The $p_\perp$ orbital of the bridging carbon is pushed up in energy because of the π^* type of interaction with the OMe group (Figure 6). Because of this, in the HOMO-1 of III, the contribution from (δ_1) is decreased and hence the antibonding nature between (δ) of Fe(2)–Fe(3) and the $p_\perp$ orbital of COMe in III (refer to Figure 3, left) also decreased. This decreases the tendency for the Fe(2)–Fe(3) axis to push the CR group to smaller dihedral angles. The curve for the sum of the 1-electron energies for the variation of θ in III shows a minimum at θ = 89.3° (the experimental value = 91°). A Walsh diagram is not very informative because of the absence of any symmetry. However a close look at the MOs shows that there is a decrease in the slope of 6a′, which indicates that III can accommodate larger dihedral angles. This idea is also supported by the calculations on $HFe_3(CO)_{10}(\mu\text{-CNH}_2)$ (**3b**). In **3b**, the energy minimum is found at θ = 93°. This is very close to the experimentally observed θ = 96.8° for $HFe_3(CO)_{10}(\mu\text{-CNMe}_2)$.[3e] The Walsh diagram for a change in θ in **3b** (Figure 5b) is very much similar to Figure 5a except for a diminished slope of 6a′. Consequently, the sum of the 1-electron energy curve shows a minimum at 93° in comparison to θ = 77° observed for **3a**.

Electronic Structure of $HOs_3(CO)_{10}(\mu\text{-CH})$ (XXI).[19] The construction of the MOs of $HOs_3(CO)_{10}(\mu\text{-CH})$ (**8a**) from smaller fragments $HOs_3(CO)_{10}$ and CH at θ = 90° is shown in Figure 3 (right). The MOs of $HOs_3(CO)_{10}$ are

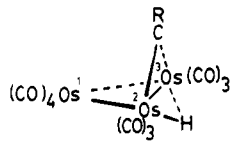

8a R = H

8b R = NH_2

Scheme III

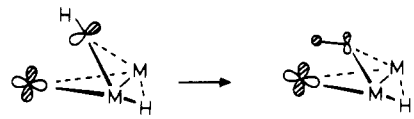

comparatively at a higher energy than those of $HFe_3(CO)_{10}$. As a result, some stronger interactions between CH and $HOs_3(CO)_{10}$ are observed. The striking difference between Figure 3 (left) and Figure 3 (right) is the three-center 2-electron interaction leading to 6a′. The antibonding interaction (π^*) between the p orbital of carbyne and the δ orbital of M(2)–M(3) is stronger in **8a** than in **3a** (Figure 3). This should lead to smaller θ in **8a** than in **3a**. The Walsh diagram in Figure 5c for $HOs_3(CO)_{10}(\mu\text{-CH})$ is qualitatively similar to Figure 5a except for the changes arising due to the higher energy of the osmium d orbitals. The variation in the sum of 1-electron energies as a function of θ in **8a** shows a minimum at 70°. This is very close to the experimentally observed θ = 69.7° for $HOs_3(CO)_{10}(\mu\text{-CH})$ (XXI). Figure 5c shows that in **8a** also the variation in θ is largely controlled by the 6a′ orbital only. In XXI also both MOs corresponding to the σ (1a′) and σ^* (6a′) interaction between Os(1) and C are occupied. This suggests that in XXI the bridging carbyne should be treated as a μ_2 bridge, even though the Os(1)–C distance is in the bonding range. This prompts us to consider XXI as a member of the group of compounds that exhibit short interatomic distances without any bonding.[26]

In the case of regular μ_3 system, **1**, the R group is bent away from M(1). The crystal structure of XXI shows that the hydrogen atom on the carbyne bridge is bent toward Os(1).[19] This originates from the antibonding Os(1)–C interaction in the HOMO-1 (6a′). To decrease this antibonding interaction, the molecule pushes the hydrogen atom of the bridging carbyne away from the Os(2)–C–Os(3) plane and toward Os(1) (Scheme III). A weak bonding interaction between Os(1) and the hydrogen of the carbyne is developed. **3a** is also expected to have an M–H interaction. On the basis of the MO analysis, we suggest that the bonding in $HOs_3(CO)_{10}(\mu\text{-CH})$ (XXI) is only η^2-μ_2 but not μ_3. Compound XXI appears to be a special case from the geometric considerations. But the electronic structure indicates a bonding interaction of the CR group with only two metals. This is at one end of the spectrum of dihedral angles observed in the compounds with the general molecular formula $HM_3(CO)_{10}(\mu\text{-CR})$.

The effect of substituents on the carbynyl carbon is clearly observed in the case of Os compounds also (Table I). The Walsh diagram (Figure 5d) for the variation of θ in $HOs_3(CO)_{10}(\mu\text{-CNH}_2)$ (**8b**) is very much similar to that of Figure 5c, the only difference being the slope of the 6a′ orbital. The curve for the sum of the 1-electron energies shows a minimum at θ = 91° for **8b** in contrast to the minimum at θ = 70° for **8a**. This is because of the decrease in the antibonding interaction between the $p_\perp$ orbital of the carbynyl carbon and the δ orbital of M(2) and M(3) as a function of R.

The above discussion of **3a** and **8a** suggests that the dihedral angle θ is dictated by the extent of the antibonding interaction observed between the M(2) and M(3) δ orbitals and the carbynyl carbon. Stronger antibonding interactions in the 6a′ orbital leads to smaller dihedral angles because smaller values of the dihedral angle help in decreasing the antibonding interaction. However this is tempered by the M(1)–C antibonding interaction. This delicate balance between the M(2)–C–M(3) and M(1)–C antibonding interactions (in 6a′ of Scheme II) controls the

dihedral angle, θ. Even though the notations μ_2 and μ_3 seem to be appropriate to describe the structure at the extremes of the spectrum of compounds from the geometric considerations, it does not still mean that the electronic structures at the extremes are similar. The carbyne group in both the extremes may be considered as bonding to two metals only.

Similar geometric preferences are expected in $HM_2M'Cp(CO)_7(\mu\text{-}CR)$, which is obtained by replacing the $M(CO)_4$ unit of **2** by the isolobal M'Cp(CO) unit. But experimental results do not support this. Complexes with the general formula $HM_2M'Cp(CO)_7(\mu\text{-}CR)$ prefer a μ_3 arrangement for the carbyne ligand. There are three of them known, all with methoxycarbyne (XXII–XXIV, Table I).[20,21] Methoxycarbyne was found to give μ_2 bonding in the "all-carbonyl" complexes (III, IX, and XV, Table I). The changes in the electronic structure that follow from a substitution of $M(CO)_4$ by MCp(CO) are analyzed below.

Electronic Structure of $HRhFe_2(CO)_7Cp(\mu\text{-}CH)$ (9). There are several trinuclear structures where three carbonyls are replaced by a Cp group (XXII–XXIV, XXVI, Table I).[20,21] All of these compounds have a short M(1)–CR distance even when the substituent R is an alkoxy group. A partial bridging nature is proposed between the unique carbonyl and two metals to account for the 18-electron count in these complexes.[20,21] We have seen that XXI also shows short M–C distances, but there is no bonding interaction to assign a μ_3-bonding mode to the CR group. Do these compounds with Cp ligands also fall into this category? Electronic structure calculations on $HRhFe_2(CO)_7(\mu\text{-}COMe)$ reported earlier[20] have indicated the presence of a clear Rh–C σ bond and μ_3 arrangement for the bridging carbyne group. We have tried to see the differences between $HFe_3(CO)_{10}(\mu\text{-}CH)$ and $HRhFe_2(CO)_7Cp(\mu\text{-}CH)$ in the following way. Figure 2 (right) shows an interaction diagram for the construction of the MOs of **9** (90°) from the fragments RhCp(CO) and $Fe_2(CO)_6$ (**5**). The MOs of RhCp(CO) are very much similar to its isolobal fragment $Fe(CO)_4$, but higher in energy. In the low symmetry of Cp(CO)Rh, t_{2g} is split into three well-separated levels. The HOMO of RhCp(CO) interacts with the LUMO of **5** to give 7a″ of **9**. The LUMO and HOMO-1 of RhCp(CO) (4a′ and 3a′) and the HOMO of **5** are involved in a three-orbital stabilizing interaction. The resultant HOMO, 6a′, of **9** is bonding between Rh and C. The corresponding orbital in **3a** (HOMO-1) is the result of a two-orbital interaction (only) that leads to Fe(1)–Fe(2) bonding and Fe(1)–C antibonding. Figure 4b shows the contour plot for the MO 6a′ of **9**. This particular bonding interaction is possible because of the directional properties and the higher energy of the MOs of Rh(CO)Cp in comparison to that of $Fe(CO)_4$.[33] Besides, there is no antibonding MO in **9** corresponding to the 3a′ MO of **3a** (i.e. antibonding between C–O and C–H bonds, Scheme II). Calculations are repeated on **9** at $\theta = 69.2°$. Figure 7 shows the correlation between the MOs of **9** at $\theta = 90°$ and $\theta = 69.2°$. The 6a′ orbital comes down in energy with the decrease in θ. 6a′ shows the Rh–C σ-bonding interaction at $\theta = 69.2°$. The overlap population between Rh and C(H) in **9** increases largely with decreasing θ (0.175 at $\theta = 90°$ and 0.354 at $\theta = 69.2°$), indicating the developing Rh–C σ bond. Therefore the carbyne group should be treated as a μ_3 bridging group. Thus the directionality of RhCp(CO) orbitals pave the way for a μ_3 arrangement for the carbyne bridge in **9**. In structures XXII–XXIV (Table I), θ is less than 70° and the M(1)–C distance indicates a μ_3 arrangement. Calculations made on **9** and $HRhFe_2Cp(CO)_7(\mu\text{-}COMe)$ (XXII) as a function of variation in θ show energy minima at $\theta = 70°$, which are very close to the experimental observation for XXII (69.2°).

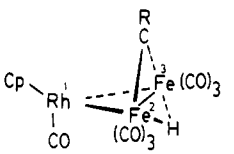

9

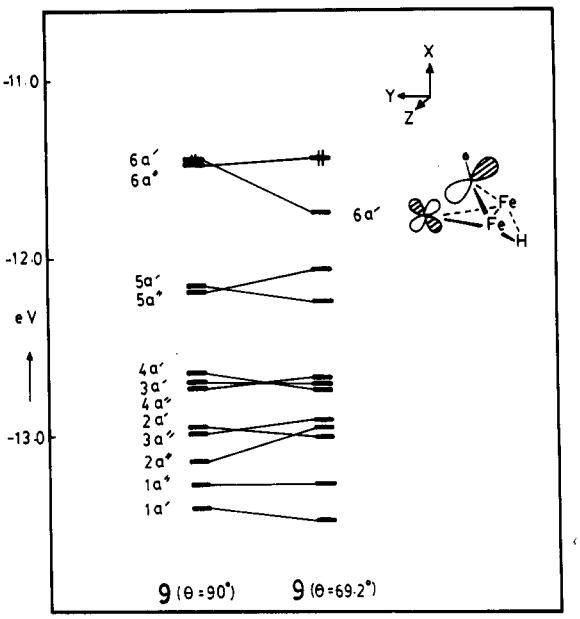

Figure 7. Correlation diagram showing correlation of the MOs of $HRhFe_2(CO)_7Cp(\mu\text{-}CH)$ at $\theta = 90°$ and at $\theta = 69.2°$.

Table II

param	3a	3b	8a	8b	9	XXI
M(1)–M(2) = M(1)–M(3), Å	2.62	2.62	2.86	2.86	2.64	2.86
M(2)–M(3), Å	2.61	2.61	2.84	2.84	2.61	2.84
M(1)–C[a], Å	2.64	2.64	2.81	2.81	2.66	2.35
M(2)–C = M(3)–C, Å	1.86	1.86	2.04	2.04	1.86	2.04
M(2)–H = M(3)–H, Å	1.62	1.62	1.62	1.62	1.62	1.62
θ,[a] deg	90.00	90.00	90.00	90.00	90.00	69.70

[a] Varies with the dihedral angle in the Walsh diagram.

Conclusions

The electronic structure of $HFe_3(CO)_{10}(\mu\text{-}CH)$ shows that the p orbital of the carbynyl carbon finds antibonding interactions with all the three metals in the HOMO-1. A delicate balance between these antibonding interactions controls the observed changes in the angle θ between the M(1)–M(2)–M(3) and M(2)–C–M(3) planes. The coefficient size on the carbon p orbital varies as a function of the R group in the carbyne bridge, which is responsible for the decrease in θ with the decreasing electron-donating nature of R. No M(2)–C–M(3) π delocalization should be expected in $HM_3(CO)_{10}(\mu\text{-}CR)$ compounds. The electronic structure of the $HMe_3(CO)_{10}(\mu\text{-}CR)$ compounds suggests only a μ_2 arrangement for the bridging carbyne, despite the short M(1)–C distance. Only a η^2–μ_2 C–H bridge but not a μ_3-CH bridge, should be expected in $HOs_3(CO)_{10}(\mu\text{-}CH)$. The directionality of the MOs of the RhCp(CO) unit in $HRhCp(CO)Fe_2(CO)_6(\mu\text{-}CR)$ is different from that of $HFe_3(CO)_{10}(\mu\text{-}CR)$ and stabilizes a μ_3 carbyne bridge.

(33) A comparison of the directional properties of MCp(CO) and $M(CO)_4$ can be found: Elian, M.; Chen, M. M. L.; Mingos, D. M. P.; Hoffmann, R. *Inorg. Chem.* **1976**, *15*, 1148.

Acknowledgment. B.V.P. thanks the Council of Scientific and Industrial Research, New Delhi, for financial support. The computations are carried at National Informatic Centre, Hyderabad.

Appendix

The important geometric parameters used for compounds **3a**, **3b**, **8a**, **8b**, and XXI are given in Table II. The Walsh diagrams (Figure 5) are constructed by varying θ from 105 to 65°. As a function of θ, the R group on the carbynyl carbon is tilted away from the M(1)-C-M(2) plane and away from M(1) so that carbyne in the compounds at a smaller dihedral angle becomes a μ_3 bridge. The position of the bridging hydrogen is varied as a function of θ. M(2)-C-M(3) vs M(2)-H-M(3) is maintained at 175°. The coordination of the carbonyls does not show any major change in II[3e] and XVII.[16] This prompted us to keep the coordination of carbonyls around the metals in the construction of the Walsh diagrams constant. Arbitrary variation of the CO ligands in such bulky molecules is not advisable because of steric reasons. The atomic parameters used for the extended Huckel calculations are taken from the literature, which suits best for the trimetallic clusters.[34,29] The weighted H_{ij} formula is used. Distances are in angstrom units, and angles are in degrees.

(34) Jorgensen, K. A.; Hoffmann, R.; Fisel, C. R. *J. Am. Chem. Soc.* **1982**, *104*, 3858.

Complexes with Unbridged Dative Bonds between Osmium and a Group 6 Element. Structures of $(OC)_{5-x}(Bu^tNC)_xOsCr(CO)_5$ (x = 1, 2)

John A. Shipley, Raymond J. Batchelor, Frederick W. B. Einstein, and Roland K. Pomeroy*

Department of Chemistry, Simon Fraser University, Burnaby, British Columbia, Canada V5A 1S6

Received August 23, 1990

The isocyanide derivatives $Os(CO)_{5-x}(Bu^tNC)_x$ (x = 1, 2) have been prepared from the reaction of $Os(CO)_5$ (or, for x = 1, $Os(CO)_4(\eta^2$-cyclooctene)) and Bu^tNC. Reaction of these derivatives with $M(CO)_5(THF)$ (M = Cr, Mo, W) in hexane yields $(OC)_{5-x}(Bu^tNC)_xOsM(CO)_5$. The structures of $(OC)_4(Bu^tNC)OsCr(CO)_5$ (**1-Cr**) and [*cis-dieq*-$(OC)_3(Bu^tNC)_2Os$]$Cr(CO)_5$ (**2b-Cr**) have been determined by X-ray crystallography: compound **1-Cr** crystallizes in the space group *Pnam* with a = 20.272 (4) Å, b = 9.648 (1) Å, c = 9.843 (2) Å, Z = 4, R = 0.027, and R_w = 0.027 for 1306 reflections ($I \geq 2.5\sigma(I)$); compound **2b-Cr** crystallizes in the space group $P2_1/n$ with a = 9.129 (1) Å, b = 12.258 (1) Å, c = 20.863 (3) Å, β = 90.32 (1)°, Z = 4, R = 0.026, and R_w = 0.022 for 2505 reflections ($I \geq 2.5\sigma(I)$). In both **1-Cr** and **2b-Cr** the 18-electron moiety $Os(CO)_{5-x}(CNBu^t)_x$ acts as a 2-electron donor ligand to the chromium atom in the $Cr(CO)_5$ unit via an unbridged, dative metal-metal bond (the Os-Cr distance is 2.966 (2) Å in **1-Cr** and 2.969 (2) Å in **2b-Cr**); the isocyanide ligands are in cis positions to the metal-metal bonds. The spectroscopic data for the $(OC)_4(Bu^tNC)OsM(CO)_5$ complexes indicate that the solid-state structure found for **1-Cr** is also adopted by these complexes in solution. There is no evidence for the isomer with the non-carbonyl ligand trans to the Os-M bond. This is in contrast to the $(R_3P)(OC)_4OsM(CO)_5$ complexes where this is the major, or only, isomer present in solution. The spectroscopic properties of the kinetically preferred products from the reaction of $Os(CO)_3(CNBu^t)_2$ with $M(CO)_5(THF)$ indicate the isocyanide ligands occupy equatorial sites on osmium that are mutually trans (i.e., [*trans-dieq*-$(OC)_3(Bu^tNC)_2Os$]$M(CO)_5$). When these complexes are stirred in CH_2Cl_2 solution at room temperature, they isomerize (over 2-10 days) to give an equilibrium mixture more concentrated in a second isomer. Spectroscopic data of pure samples of the second isomer indicate the Bu^tNC ligands are in equatorial positions on the osmium atom that are mutually cis (as indicated above, this was confirmed by X-ray crystallography for the chromium compound). Once again, there was no evidence for the isomer with an isocyanide ligand trans to the metal-metal bond.

Introduction

Work from this laboratory over the past 7 years has demonstrated that neutral, 18-electron metal carbonyl compounds can act as ligands. Some examples of complexes with this type of ligand are $(OC)_5OsOs(CO)_3(GeCl_3)(Cl)$,[1] $(\eta^5$-$C_5Me_5)(OC)_2IrW(CO)_5$,[2] and $(Me_3P)(OC)_4OsRe(CO)_4(Br)$.[3] The metal-metal bonds in these complexes are donor-acceptor (dative) bonds, and as shown by X-ray crystallography, they are unbridged.

In a recent paper we described the preparation of complexes of the type $(R_3P)(OC)_4OsM(CO)_5$ (M = Cr, Mo, W).[4] The X-ray crystal structures of $(Me_3P)(OC)_4OsCr(CO)_5$ and its tungsten analogue revealed that the metal-metal bond is also unbridged with the phosphine ligand trans to the metal-metal bond. Carbon-13 NMR spectroscopy demonstrated that the isomer with the PR_3 ligand trans to the Os-M bond was also the major isomer present for these complexes in solution. For the complexes that had phosphorus ligands with a small cone angle, there were, however, significant amounts of the isomer with the PR_3 ligand cis to the Os-M bond present.[4]

(1) Einstein, F. W. B.; Pomeroy, R. K.; Rushman, P.; Willis, A. C. *J. Chem. Soc., Chem. Commun.* **1983**, 854.
(2) Einstein, F. W. B.; Pomeroy, R. K.; Rushman, P.; Willis, A. C. *Organometallics* **1985**, *3*, 250.
(3) Einstein, F. W. B.; Jennings, M. C.; Krentz, R.; Pomeroy, R. K.; Rushman, P.; Willis, A. C. *Inorg. Chem.* **1987**, *26*, 1341.
(4) Davis, H. B.; Einstein, F. W. B.; Glavina, P. G.; Jones, T.; Pomeroy, R. K.; Rushman, P. *Organometallics* **1989**, *8*, 1030.

0276-7333/91/2310-3620$02.50/0